Spectrochimica Acta Part A: Molecular and Biomolecular Spectroscopy 261 (2021) 120055

Contents lists available at ScienceDirect

Spectrochimica Acta Part A: Molecular and Biomolecular Spectroscopy

journal homepage: www.elsevier.com/locate/saa

# A long-wavelength fluorescent probe with a large Stokes shift for lysosome-targeted imaging of Cys and GSH

Yi-Hang Sun [a,1], Hai-Hao Han [a,b,1], Jia-Min Huang [a], Jia Li [b], Yi Zang [b,*], Cheng-Yun Wang [a,*]

[a] Key Laboratory for Advanced Materials and Institute of Fine Chemicals, School of Chemistry and Molecular Engineering, East China University of Science & Technology, Shanghai 200237, PR China

[b] National Center for Drug Screening, State Key Laboratory of Drug Research, Shanghai, Institute of Materia Medica, Chinese Academy of Sciences, 189 Guo Shoujing Rd., Shanghai 201203, PR China

## HIGHLIGHTS

- Near-Infrared fluorescent probe with a large Stokes shift (180 nm).
- High selectivity, low detection limit and rapid response for Cys and GSH.
- Low toxicity and precise locating at lysosomes in HepG2 cells.
- Aromatic morpholine as the lysosome-targeting agent.

## GRAPHICAL ABSTRACT

A long-wavelength fluorescent probe with a large Stokes shift for lysosome-targeted imaging of Cys and GSH.

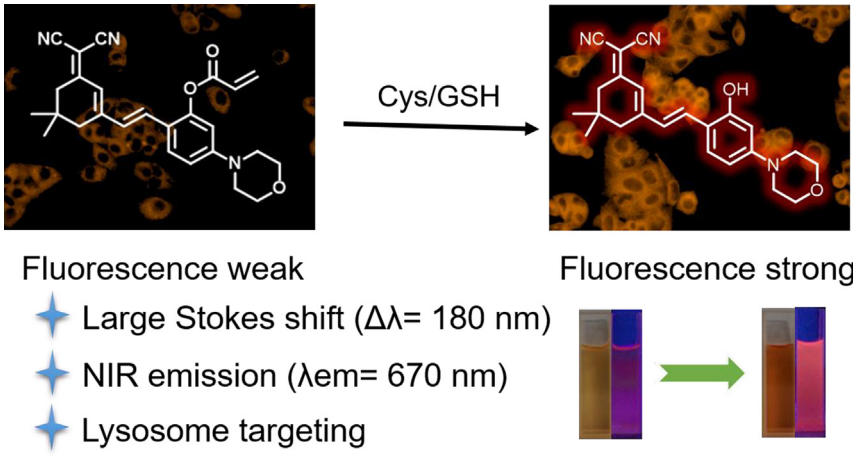


## ARTICLE INFO

*Article history:*
Received 4 April 2021
Received in revised form 24 May 2021
Accepted 2 June 2021
Available online 5 June 2021

*Keywords:*
Fluorescent probe
Lysosome targeting
Cysteine
Glutathione
Near Infrared Emission
Bioimaging

## ABSTRACT

Biothiols including cysteine (Cys) and glutathione (GSH) are biological signaling molecules responsible for cell detoxification, cell metabolism and neutralization of reactive oxygen species. Here, we synthesized a long-wavelength fluorescent probe, **DCIMA**, for lysosome-targeted imaging of Cys and GSH in living cells. **DCIMA** is consisted of a dicyanoisophorone core modified with an acrylate group for biothiol detection through the Michael addition reaction and a morpholine group as the lysosome-targeting agent. The presence of the electron-donating morpholine group also enhances the intramolecular charge transfer mechanism of the probe, thereby enabling its long-wavelength fluorescence emission (670 nm) and large Stokes shift (180 nm). In concentration range of 0–30 μM, the probe was determined to react quickly with both Cys and GSH with low detection limits (<5 min, 35.2 nM for GSH and 34.8 nM for Cys) and achieve the sensitive fluorescence imaging of the biothiols located in the lysosomes of living cells.



* Corresponding authors.
*E-mail addresses:* yzang@simm.ac.cn (Y. Zang), cywang@ecust.edu.cn (C.-Y. Wang).

[1] These authors contributed equally to this work.

https://doi.org/10.1016/j.saa.2021.120055
1386-1425/

## 1. Introduction

Cysteine (Cys) and glutathione (GSH) are important biothiols implicated in a number of biological processes [1,2]. They are responsible for balancing intracellular redox processes, modulating cell metabolism and detoxification, and facilitating protein synthesis [3–5]. While the lack of Cys can lead to skin lesions, neurotoxicity, edema and liver damage, the excess of which may cause cardiovascular and Parkinson's disease [6–8]. In the meanwhile, GSH, which is consisted of glutamic acid, cysteine and glycine, [9] contributes to the redox balance of cells by eliminating intracellular reactive oxygen species (ROS). The decrease of GSH is an early activation signal of cell apoptosis [10]. Intracellular Cys and GSH concentration is closely related to biosynthesis and a variety of human diseases [11]. Recent studies suggest that lysosomal Cys and GSH play an important role in digesting and metabolizing intracellular substances [12,13]. As a result, sensitive analytical tools that can effectively detect and quantify Cys and GSH at the subcellular level is of significance for basic biomedical research and disease diagnosis [14,15].

Fluorescent probes, owing to their synthetic simplicity, highly tunable photophysical properties and superior sensitivity to many other existing analytical agents, have become the technique of choice for biosensing and bioimaging of biothiols [16,17]. The sensing mechanisms include cyclization with aldehydes, [18–20] conjugate addition-cyclization with acrylates, [21–23] Michael addition, [24–26] aromatic substitution-rearrangement reaction, [27,28] cleavage of sulfonamide, [29–31] sulfonate ester [32,33] and superimposed applications of the above methods [34,35]. Among them, acrylate reacts quickly and selectively with biothiols, and has become a popular reactive group for the construction of biothiol probes [36–40]. However, problems remain for the majority of the reported biothiol probes in terms of a short emission wavelength (<600 nm), small Stokes shift (<100 nm), relatively long response time (>10 min), and the inability to precisely localize biothiols at the subcellular level [41–43]. For lysosome localization, alkane-linked morpholine groups are frequently used, whereas the use of aromatic amines for lysosome targeting has been much less explored [44–46]. With the development of detection technology, some lysosomal localization probes with morpholine have been able to achieve near-infrared emission (650 nm ~ 800 nm) [21,47] The limit of detection has reached the nM level (5 nM ~ 200 nM) [27,48] and the response time is also accelerating (5 min ~ 15 min) [22,36]. Probes with these properties have better development potential in the field of biological detection. (**Table S1**)

Here, we synthesized a simple fluorescent probe, **DCIMA**, for lysosome-targeted imaging of Cys and GSH in live cells. Dicyanoisophorone with a long conjugated double bond was constructed to endow **DCIMA** with a long-wavelength emission and large Stokes shift. Morpholine was used to serve as both a lysosome-targeting and electron-donating group to enable a "push–pull" effect, enhancing the emission wavelength of the probe by the intramolecular charge transfer (ICT) mechanism. The response time of **DCIMA** was determined to be within 5 min to Cys and GSH with a large Stokes shift (180 nm), which is beneficial for bioimaging applications. The probe also showed excellent lysosomal localization effect and low detection limits (35.2 nM for GSH and 34.8 nM for Cys, respectively).

## 2. Experiment sections

### 2.1. Materials and instruments

All reagents and solvents used in this work were purchased commercially. All UV–vis and fluorescence spectra were measured on CARY Eclipse spectrophotometer and Varian Cary 500 spectrophotometer, respectively. $^1$H NMR and $^{13}$C NMR spectra were obtained by Bruker AM-400 and Ascend 600 spectrometer. Waters LCT Permier XE spectrometer was used to measure high-resolution mass spectra, and a pH-10C digital pH meter was used to measure pH.

### 2.2. Synthesis

Synthesis of compound **1** and **2** was described in **supporting information (Fig. S1, S2)**.

Synthesis of **DCIMH**: Compound **2** (1 mmol., 0.207 g) and dicyanoisophrone (1 equiv, 0.186 g) were mixed in MeCN (10 mL) in a round bottom flask with rigorous stirring. The reaction solution was refluxed for 12 h, and then the solvent was removed under reduced vacuum. The residue was purified by column chromatography ($CH_2Cl_2$) to produce a deep-red solid (**DCIMH**) (0.150 g, yield: 40%). $^1$H NMR (400 MHz, Chloroform-d) $\delta$ 7.42 (d, $J$ = 8.8 Hz, 1H), 7.33 (d, $J$ = 16.1 Hz, 1H), 6.97 (d, $J$ = 16.1 Hz, 1H), 6.75 (s, 1H), 6.50 (dd, $J$ = 8.8, 2.2 Hz, 1H), 6.30 (d, $J$ = 2.1 Hz, 1H), 3.86–3.83 (t, $J$ = 4.8 Hz, 4H), 3.25–3.20 (t, $J$ = 4.8 Hz, 4H), 2.56 (s, 2H), 2.47 (s, 2H), 1.06 (s, 6H). $^{13}$C NMR (151 MHz, $CDCl_3$) $\delta$ 187.85, 169.43, 160.93, 156.39, 155.88, 132.70, 129.04, 126.14, 121.75, 107.96, 66.59, 47.89, 46.93, 40.72, 26.60, 24.72. HRMS (ESI): $m/z$ Calcd. for $C_{23}H_{26}N_3O_2$ ([M + H]$^+$): 376.2025; Found 376.2029 (Fig. S3-5).

Synthesis of **DCIMA**. **DCIMH** (1 mmol, 0.375 g) and $Et_3N$ (2 equiv., 0.200 g) were mixed in dry $CH_2Cl_2$ (10 mL) in a round bottom flask. Then, acryloyl chloride (2 equiv., 0.180 g) was added at 0 °C dropwise, and the reaction was proceeded at room temperature. After stirring for 6 h, the mixture was poured into ice water. The resulting crude product was extracted with $CH_2Cl_2$ (20 mL × 3), and solvent was removed by vacuum evaporation. The residue was purified by column chromatography ($CH_2Cl_2$) to produce a dark-orange solid (**DCIMA**) (0.197 g, yield: 46%). $^1$H NMR (600 MHz, DMSO $d_6$) $\delta$ 7.83 (d, $J$ = 8.7 Hz, 1H), 7.24 (d, $J$ = 16.0 Hz, 1H), 7.00 (d, $J$ = 16.1 Hz, 1H), 6.94 (d, $J$ = 8.2 Hz, 1H), 6.80 (s, 1H), 6.76 (s, 1H), 6.61 (d, $J$ = 17.2 Hz, 1H), 6.55–6.47 (m, 1H), 6.22 (d, $J$ = 10.1 Hz, 1H), 3.72 (s, 4H), 3.26 (s, 4H), 2.58 (s, 2H), 2.42 (s, 2H), 0.99 (s, 6H).$^{13}$C NMR (151 MHz, $CDCl_3$) $\delta$ 169.16, 164.31, 154.32, 152.73, 150.29, 133.53, 130.09, 128.00, 127.70, 127.45, 122.86, 118.84, 113.77, 112.98, 112.83, 108.20, 66.52, 47.75, 43.01, 39.01, 31.99, 28.04. HRMS (ESI): $m/z$ Calcd. for $C_{26}H_{27}N_3O_3Na$ ([M + Na]$^+$): 452.1950; Found 452.1948 (**Fig. S6-S8**).

### 2.3. Spectroscopic properties test

Stock solution of **DCIMA** (1.0 mM) was prepared in DMSO. Biomolecules including Cysteine (Cys), homocysteine (Hcy), glutathione (GSH), alanine (Ala), Arginine (Arg), asparagine (Asn), glutamine (Gln), glutamic acid (Glu), glycine (Gly), histidine (His), lysine (Lys), methionine (Met), phenylalanine (Phe), proline (Pro), threonine (Thr), tyrosine (Tyr), valine (Val) and anions ($S_2O_3^{2-}$, $HSO_3^-$, $HS^-$, $SO_4^{2-}$) were prepared in distilled water at 10 mM. **DCIMA** (10 μM) were prepared by stock solution (1.0 mM) and DMSO/PBS (1:4, v/v, pH 7.4), and then different analyte stock solutions (10 mM) were added to determine the responsiveness of **DCIMA**. The limit of detection was calculated by 3σ/k, Cys or GSH stock solutions were added to **DCIMA** (10 μM) incrementally for quantitative detection, and k was obtained by calculating the slope of linear fitting. For interference study, **DCIMA** (10 μM) was incubated with 15 μL competing species stock solutions (50 μM) for 10 min. Then Cys (50 μM) were added to confirm the anti-interference ability. All spectroscopic measurements were

carried out in a mixture of DMSO/PBS (phosphate buffered saline) (1:4, v/v, pH 7.4).

### 2.4. Fluorescence imaging of cells

Cell Culture and Cell Viability Assay are shown in **supporting information**. Hep-G2 cells were seeded on a black 96-well microplate with optically clear bottom (Greiner bio-one, Germany) overnight. To detect GSH or Cys exogenously, the cells were first incubated with **DCIMA** (5 μM, 1% DMSO in PBS, pH 7.4) for 30 min, followed by incubation with GSH (1 mM) or Cys (1 mM) for 30 min. To further confirm the response of probe to exogenous GSH or Cys, the cells were pre-incubated with NEM (100 μM), a kind of biothiol Scavenger, for 0.5 h and followed by the **DCIMA** (5 μM, 1% DMSO in PBS, pH 7.4) for 30 min at 37 °C. Then, cells were washed with PBS (phosphate buffered saline) three times. The fluorescence images were recorded using an Operetta high-content imaging system (Perkinelmer, US) and quantified and plotted by Columbus analysis system (Perkinelmer, US).

### 2.5. Co-localization experiment

Cells cultured in growth medium supplemented with 10% FBS were added to a 24-well microplate. Cells were maintained in a humidified atmosphere of 5% $CO_2$ and 95% air at 37 °C overnight. Then, cells were incubated sequentially with **DCIMA** (5 μM, 1% DMSO in PBS, pH 7.4) and LysoTracker (500 nM) for 30 min, and the cells on the microplate were rinsed with warm PBS and fixed with 4% paraformaldehyde for 20 min at room temperature. Immediately after sealing, the fluorescence was detected and photographed with confocal laser scanning microscopy (Leica TCS SP8, Leica Microsystems, Wetzlar, Germany red channel excitation at 488 nm, emission at 630–710 nm; Lyso tracker channel excitation at 559 nm, emission at 575–600 nm).

## 3. Results and discussion

### 3.1. Design and synthesis of DCIMA

The synthetic procedures for **DCIMA** are shown in Scheme 1. p-Hydroxyanaline and bis(chloroethyl) ether underwent an amine substitution reaction followed by cyclization to form the aromatic morpholine. Then, Vilsmeier-Haack reaction is proceeded to introduce m-aldehyde to the core structure, thereby forming the salicylaldehyde structure. **DCIMH** was obtained via a Knoevenagel reaction with piperidine as catalyst at 80 °C overnight in MeCN. Finally, **DCIMH** reacted with acryloyl chloride in dry DCM in the presence of triethylamine as an acid-binding agent to obtain **DCIMA**.

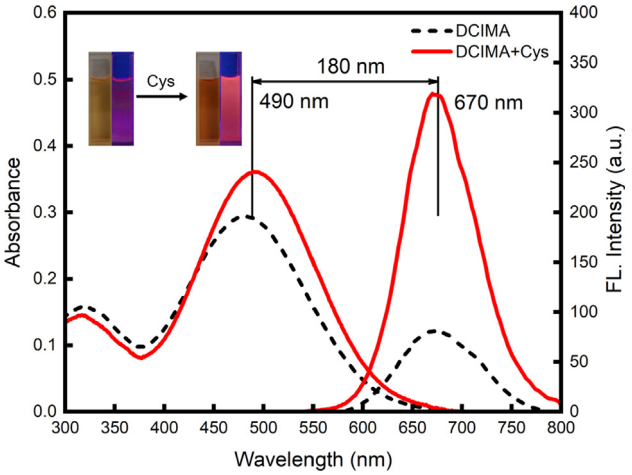


**Fig. 1.** Absorption and emission spectra of **DCIMA** (10 μM) without and with 5 equiv. of Cys in DMSO/PBS buffer (10 mM, 1:4, pH 7.43), $\lambda_{ex}$ = 490 nm Slit width: 5 nm/10 nm.

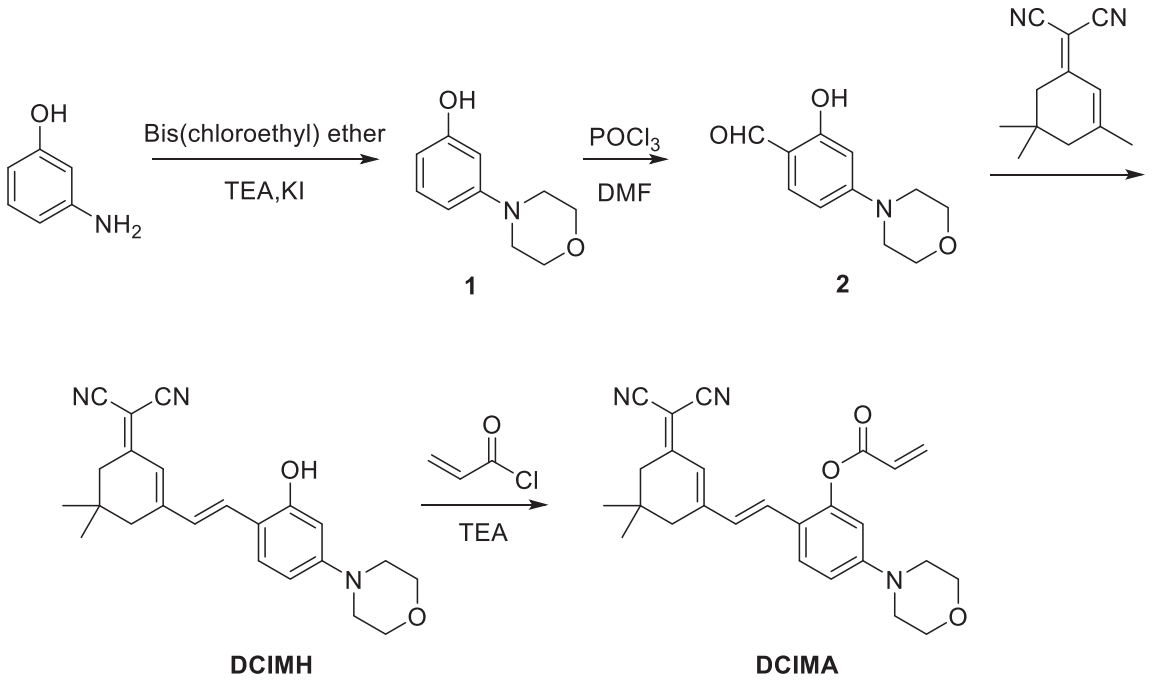


**Scheme 1.** Synthesis of **DCIMA**.

### 3.2. Spectroscopic properties of DCIMA

With the probe in hand, we tested the photophysical properties of **DCIMA** in a mixture of DMSO/PBS (1/4, v/v, pH 7.4). We observed that **DCIMA** exhibited a strong absorption peak at 460 nm. After the addition of 5 equiv. of Cys, a red-shifted absorption peak of the probe to 490 nm was observed. By excitation with 490 nm light, a fluorescence maximum at 670 nm was recorded for **DCIMA** with a 4-fold enhancement in fluorescence intensity. We note that a large Stokes shift of 180 nm was obtained for **DCIMA**, which is promising for bioimaging applications because the self-absorption of the probe and biological background fluorescence can be diminished (Fig. 1).

### 3.3. Detection of biothiols using DCIMA

Next, we turned our attention to testing the biothiol sensing properties of **DCIMA** (10 μM). Common biological competing species including Cys, Hcy, GSH, Ala, Arg, Asn, Gln, Glu, Gly, His, Lys, Met, Phe, Pro, Thr, Tyr, Val and anions ($S_2O_3^{2-}$, $HSO_3^-$, $HS^-$, $SO_4^{2-}$) were used. We determined that the fluorescence of **DCIMA** enhanced significantly in the presence of Cys and GSH, and showed a much weaker response to Hcy. In contrast, almost no fluorescence change was observed for other competing species tested (Fig. 2). In addition, the co-incubation of Cys with the competing species did not cause the fluorescence enhancement of **DCIMA** to be interfered, suggesting the good selectivity

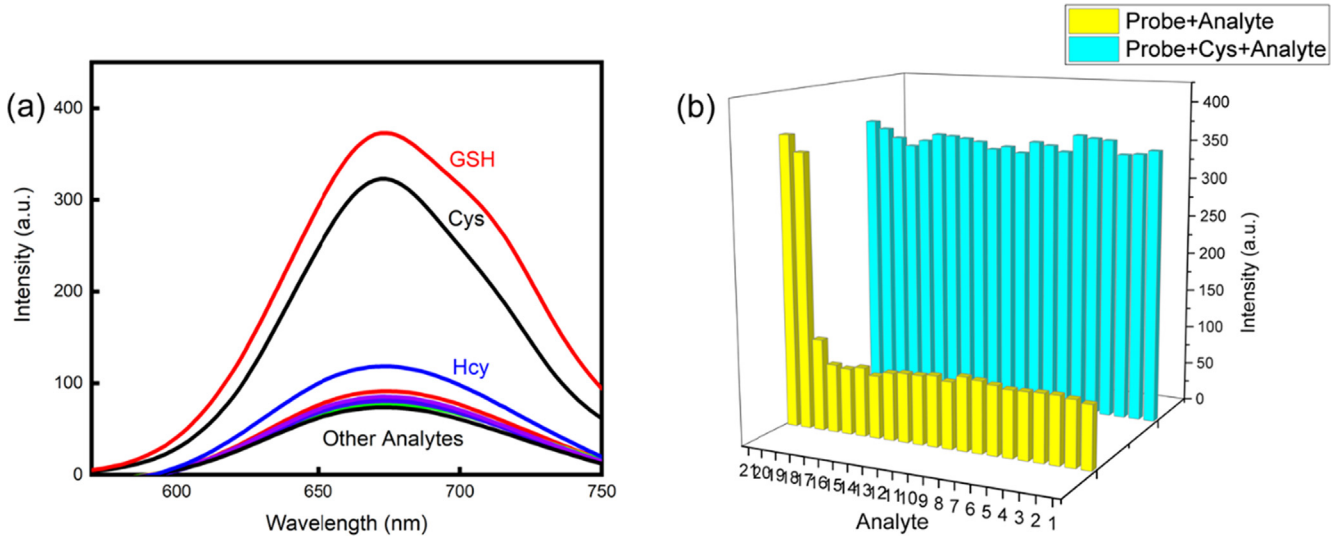


**Fig. 2.** (a) Stacked fluorescence spectra of **DCIMA** (10 μM) in the presence of different indicated analytes (50 μM); (b) Fluorescence intensity of **DCIMA** (10 μM) in the presence of different analytes (50 μM) with and without Cys (50 μM) in DMSO/PBS buffer (10 mM, 1:4, v/v, pH 7.4). 1. Ala, 2. Arg, 3. Asn, 4. Gln, 5. Glu, 6. Gly 7. His, 8. Lys, 9. Met, 10. Phe, 11. Pro, 12. Thr, 13. Tyr, 14. Val, 15. $S_2O_3^{2-}$, 16. $HSO_3^-$, 17. $HS^-$, 18. $SO_4^{2-}$, 19. Hcy, 20. Cys, 21.GSH.

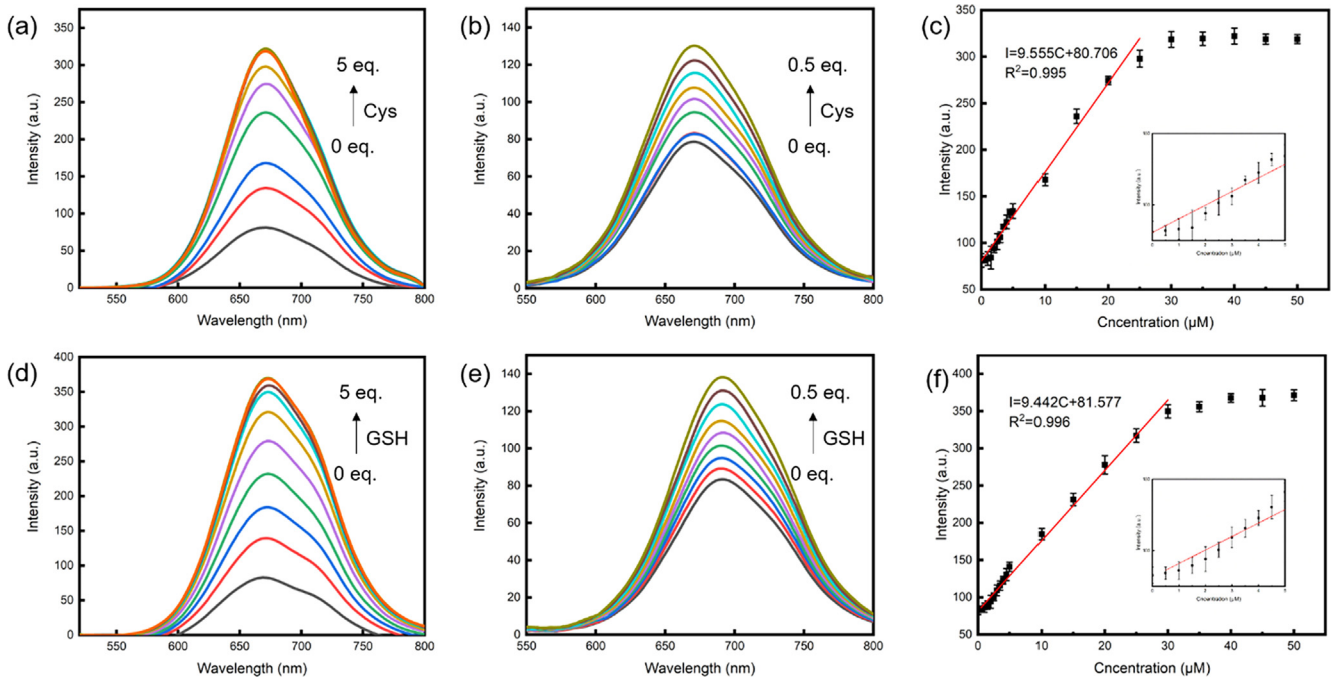


**Fig. 3.** Fluorescence titration of **DCIMA** with increasing Cys and GSH. (a, b/d, e) **DCIMA** was reacted with indicated concentrations of Cys/GSH at room temperature; (c, f) Plotting the fluorescence intensity change of **DCIMA** as a function of increasing Cys and GSH (0–50 μM). Slit width:5 nm/10 nm, $\lambda_{ex}$ = 490 nm, $\lambda_{em}$ = 670 nm.

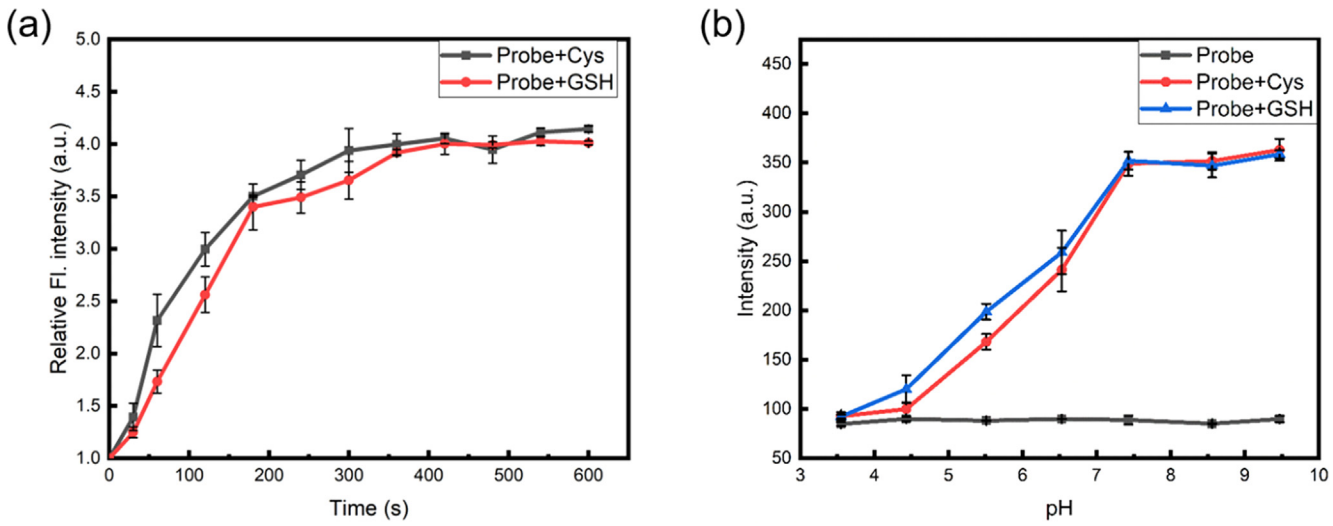


**Fig. 4.** (a) Plotting the relative fluorescence intensity of **DCIMA** (10 μM) at 670 nm with increasing GSH (50 μM) and Cys (50 μM) in DMSO/PBS (1/4, v/v, pH 7.4). (b) Plotting the fluorescence intensity of **DCIMA** (10 μM) with Cys (50 μM) and GSH (50 μM) with increasing pH.

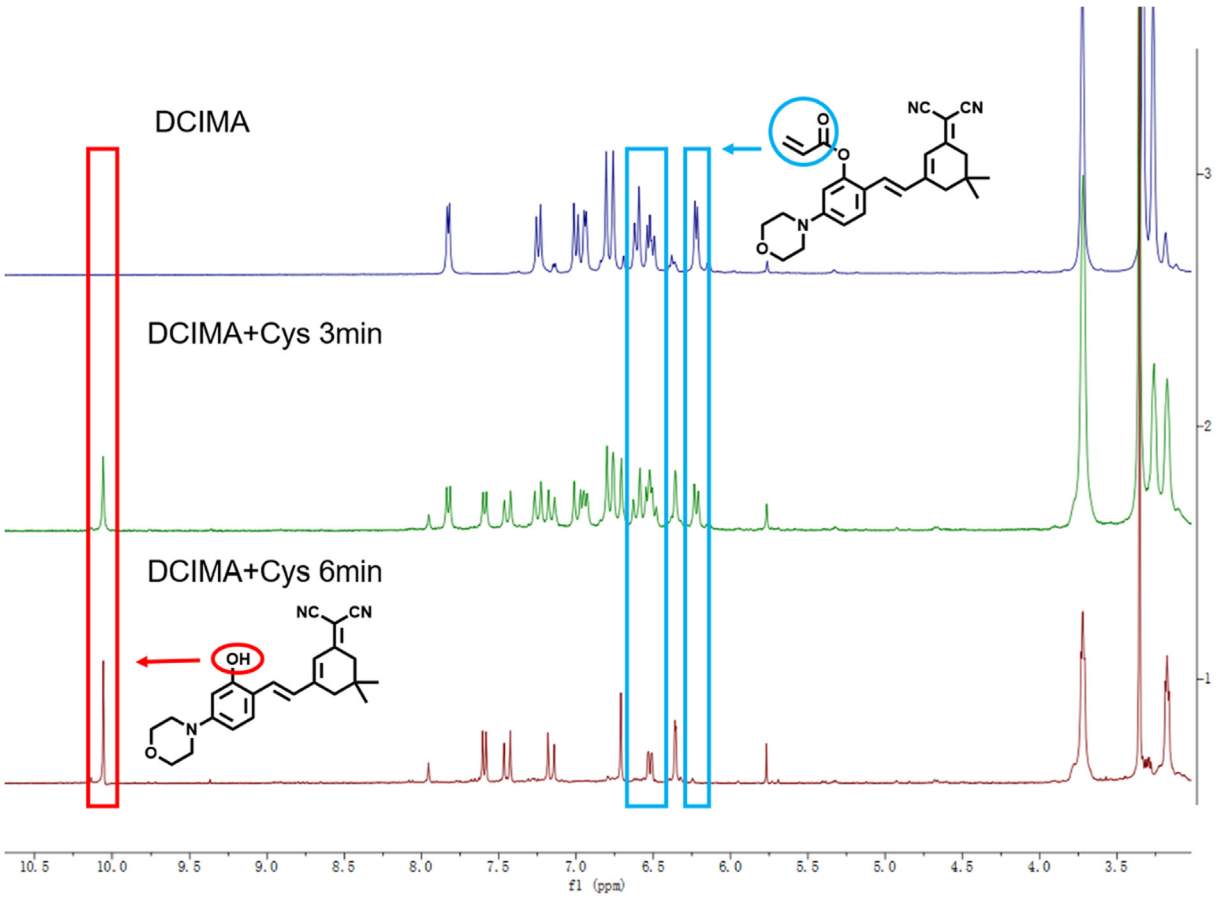


**Fig. 5.** Time-dependent $^{1}$H NMR titration of **DCIMA** with Cys in DMSO $d_6$.

of the probe for biothiol detection in a complex biological environment.

### 3.4. Quantitative detection of GSH and Cys using DCIMA

Next, we attempted whether our probe could be used for the quantitative analysis of biothiols. **DCIMA** (10 μM) was prepared in DMSO/PBS buffer (1:4, v/v, pH 7.4), followed by the addition of increasing Cys and GSH. After an incubation for 30 min at room temperature, we obtained a good linearity by plotting the fluorescence enhancement of the probe with both Cys and GSH over a concentration range of 0–30 μM (Fig. 3). The limit of detection (LOD) of **DCIMA** to Cys and GSH was determined to be 34.8 nM and 35.2 nM, respectively ($3\sigma/k$, k is the slop of linear calibration curve and k is the standard deviation). This suggests the good sensitivity of **DCIMA** for biothiol detection.

### 3.5. Reaction time and pH stability of DCIMA

To test the response time of the probe to biothiols, **DCIMA** (10 μM) was incubated with Cys and GSH (50 μM) for 10 min. We observed that equilibrium was reached within 5 min for both Cys and GSH (Fig. 4 (a)). This suggests a fast reaction kinetics of our probe for biothiols in aqueous solution, which is beneficial for cell-based experiments. We also determined that the probe

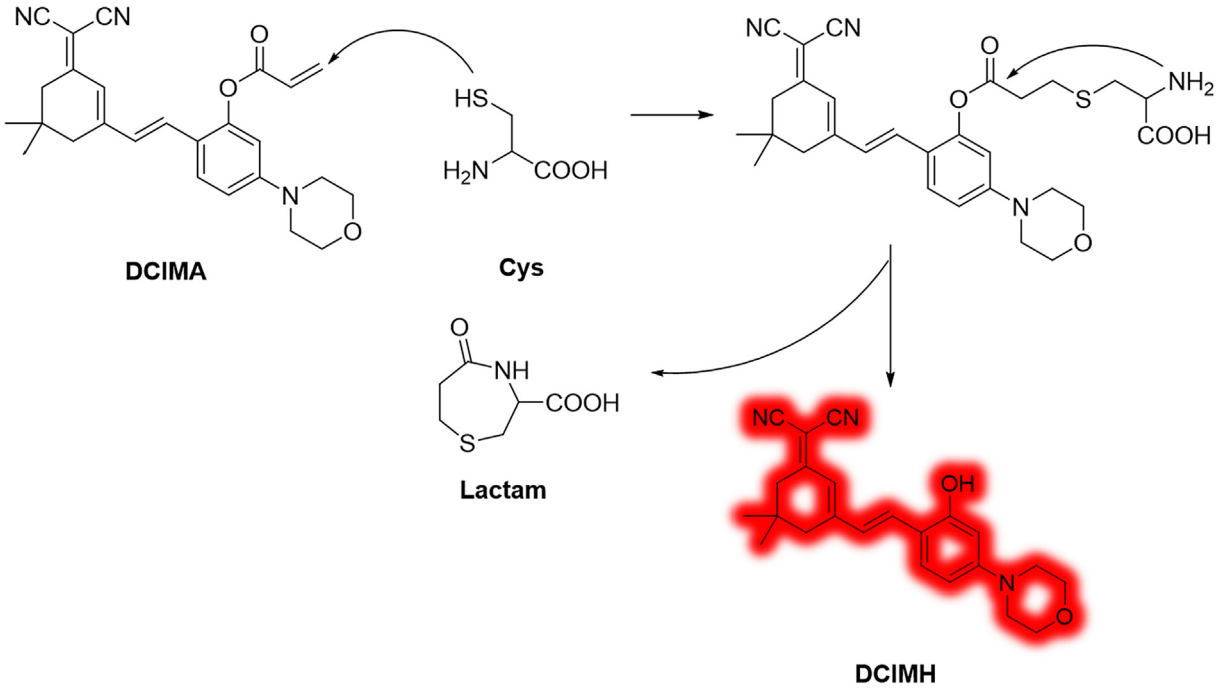


**Scheme 2.** Sensing mechanism of **DCIMA** for Cys.

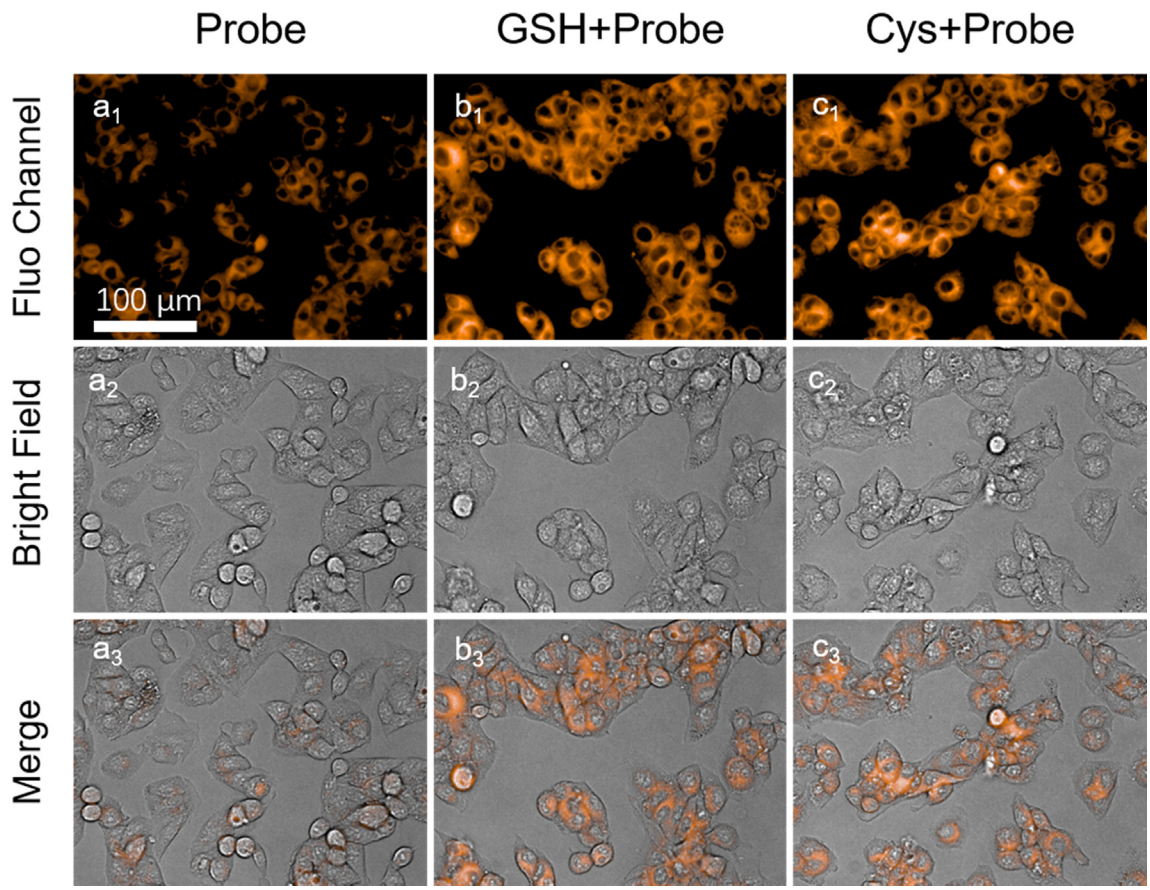


**Fig. 6.** Fluorescence imaging of exogenous biological thiols in living Hep-G2 cells. Hep-G2 cells were incubated with **DCIMA** (5 μM) without or with a subsequent addition of GSH or Cys (1 mM).

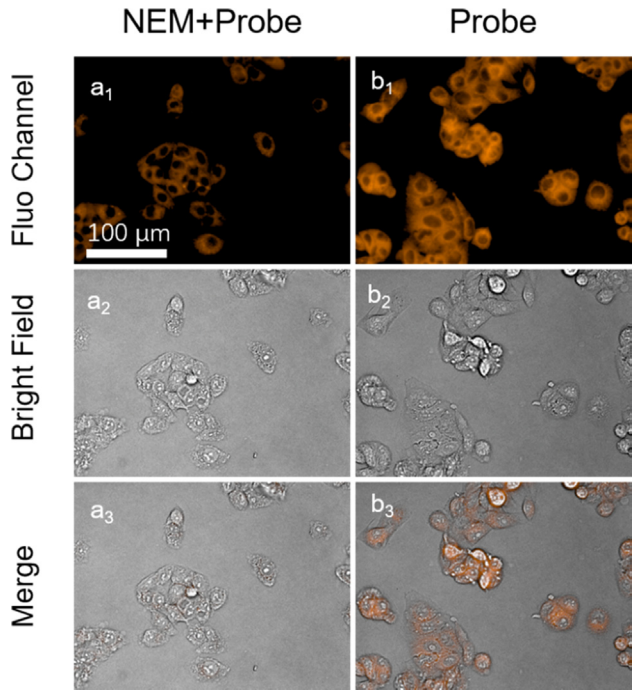


**Fig. 7.** Fluorescence imaging of endogenous biological thiols in living Hep-G2 cells. Hep-G2 cells were incubated with **DCIMA** (5 μM) in the absence and presence of NEM (100 μM) for 30 min.

responded to both Cys and GSH within a broad pH range of 3.6 to 7.4 in 5 min (Fig. 4 (b)). Although the sensitivity of the probe decreased with decreasing pH, appreciable detection signals existed at pH > 4, suggesting the applicability of the probe for imaging of biothiols in the lysosomes (pH > 4) of cells.

### 3.6. Reaction mechanism of DCIMA with biothiols

Acrylate group has been widely reported as a reactive group for Cys and other biothiols, with the ability for fluorescence quenching. After removal of the acrylate group, the suppressed electron-donating ability of hydroxyl group is reactivated. Cys reacts with acrylate group to form a seven-membered thioether intermediate by conjugate addition and intramolecular cyclization (Scheme 2). Using high-resolution mass spectrum, we determined that after the addition of 5 equiv. of Cys, the molecular ionic peak at 430.2130 of **DCIMA** decreased, and a new peak at 376.2010 appeared. This suggests that Cys contributed to the removal of acrylate group to produce **DCIMH** (**Fig. S9**). Meanwhile, HRMS also proved that **DCIMA** had a similar mechanism with GSH (**Fig. S10**). Moreover, a time-dependent $^1$H NMR experiment was also carried out (Fig. 5). With the addition of 5 equiv. of Cys, the hydroxyl proton peak at 10.05 ppm appeared, and aromatic proton signals corresponding to **DCIMA** and **DCIMH** were observed. The proton signals assigned to the acrylic group of **DCIMA** completely disappeared with the complete emergence of **DCIMH** peaks in 6 min.

### 3.7. Biothiol imaging in living cells using DCIMA

Eventually, probe **DCIMA** was used for biothiol imaging in living Hep-G2 cells (human hepatoma cell line). The cytotoxicity of the probe was first tested by an MTS cell viability assay. With a concentration range of 0–40 μM, cells were observed to be generally viability with a viability as low as 95% after 12 h (**Fig. S11**). Then, we tested the ability of **DCIMA** to image exogenous and endogenous Cys and GSH in Hep-G2 cells. Cells were incubated with 5 μM of **DCIMA** for 30 min, and then exogenous GSH or Cys (1 mM) was added. After incubation for 30 min, a significant fluorescence enhancement was observed with a fluorescence microscope (Fig. 6). Since biothiols are endogenously overexpressed at high levels in tumor cells, N-ethylmaleimide (NEM, a known biothiol scavenger, 100 μM) was used to pre-incubate with the cells for 30 min, followed by addition of **DCIMA** (5 μM). Comparing to the group without treatment with NEM, the fluorescence intensity of the cells pre-treated with NEM produced a much weaker imaging capacity (Fig. 7). This suggests that the fluorescence enhancement of the probe was dependent on intracellular biothiol concentration.

Then, we examined the subcellular localization of probe **DCIMA** by using a commercial LysoTracker for fluorescence co-localization. Hep-G2 cells were incubated with **DCIMA** (5 μM) and LysoTracker (0.5 μM) for 30 min. As shown in Fig. 8, a good overlap of the red fluorescence of **DCIMA** and the green fluorescence of the tracker was observed with a high Pearson's Correlation Coefficient of 0.98. This suggests that probe **DCIMA** can be used for fluorescence-based localization of biothiols at the subcellular level.

## 4. Conclusion

We have designed and synthesized a lysosome-targeted long-wavelength probe **DCIMA** for selective sensing of Cys and GSH in the presence of other competing species. The probe showed a long-wavelength fluorescence emission (670 nm) and large Stokes shift (180 nm) with biothiols. A fast response time (5 min) and high sensitivity (34.8 nM for Cys and 35.2 nM for GSH) were also obtained for the probe with good linear sensing range from 0 to 30 μM. Cellular experiments showed that the probe had good lysosome-targeting ability for the imaging of both exo- and endogenous biothiols. **DCIMA** possesses potential application to reveal the change of lysosomal biothiol concentration, which indi-

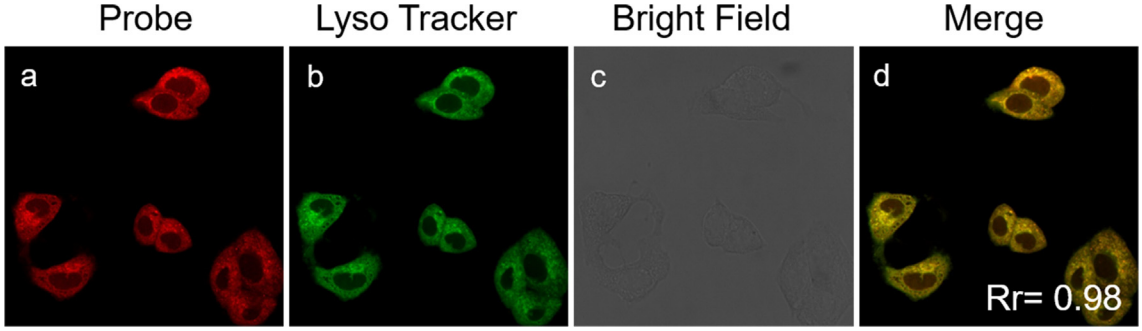


**Fig. 8.** Colocalization of probe fluorescence and Lyso-Tracker fluorescence in Hep-G2 cells. (a) Probe imaging channel (630–710 nm), $\lambda_{ex}$ = 488 nm. (b) Lyso-Tracker imaging channel (575–600 nm), $\lambda_{ex}$ = 559 nm; (c) Bright field. (d) The merged image of the fluorescence channel of probe and that of Lyso-Tracker.

cates that the probe could be used in the research on the effects of biothiols in lysosomes and related diseases.

## CRediT authorship contribution statement

**Yi-Hang Sun:** Conceptualization, Methodology, Investigation, Data curation, Visualization, Writing - original draft. **Hai-Hao Han:** Visualization, Data curation. **Jia-Min Huang:** Investigation, Data curation. **Jia Li:** Visualization, Writing - review & editing. **Yi Zang:** Supervision, Visualization, Writing - review & editing. **Cheng-Yun Wang:** Resources, Conceptualization, Supervision, Writing - review & editing, Funding acquisition.

## Declaration of Competing Interest

The authors declare that they have no known competing financial interests or personal relationships that could have appeared to influence the work reported in this paper.

## Acknowledgements

The authors are grateful for financial support from the Natural Science Foundation of Shanghai (No. 16ZR1408000) and the Fundamental Research Funds for the Central Universities.

## Appendix A. Supplementary material

Supplementary data to this article can be found online at https://doi.org/10.1016/j.saa.2021.120055.

## References

[1] D.M. Townsend, K.D. Tew, H. Tapiero, The importance of glutathione in human disease, Biomed. Pharmacother. 57 (2003) 145–155.
[2] P. Nagy, M.T. Ashby, Reactive Sulfur species: kinetics and mechanisms of the oxidation of cysteine by hypohalous acid to give cysteine sulfenic acid, J. Am. Chem. Soc. 129 (2007) 14082–14091.
[3] L.A. Herzenberg, S.C.D. Rosa, J.G. Dubs, M. Roederer, M.T. Anderson, S.W. Ela, S. C. Deresinski, L.A. Herzenberg, Glutathione deficiency is associated with impaired survival in HIV disease, Proc. Natl. Acad. Sci. USA 94 (1997) 1967–1972.
[4] A. Bindoli, J.M. Fukuto, H.J. Forman, Thiol chemistry in peroxidase catalysis and redox signaling., Antioxid Redox Signal, Antioxid. Redox Signaling 10 (2008) 1549–1564.
[5] T.P. Dalton, H.G. Shertzer, A. Puga, Regulation of gene experession by reactive oxygen, Annu. Rev., Pharmacol. Toxicol. 39 (1999) 67–101.
[6] S.R. Danielson, J.M. Held, M. Oo, R. Riley, B.W. Gibson, J.K. Andersen, Quantitative mapping of reversible mitochondrial Complex I cysteine oxidation in a Parkinson disease mouse model, J. Biol. Chem. 286 (2011) 7601–7608.
[7] H. Peng, W. Chen, Y. Cheng, L. Hakuna, R. Strongin, B. Wang, Thiol reactive probes and chemosensors, Sensors 12 (2012) 15907–15946.
[8] B. Ma, F. Zeng, X. Lia, S. Wu, A facile approach for sensitive, reversible and ratiometric detection of biothiols based on thymine-mediated excimer-monomer transformation, Chem. Commun. 48 (2012) 6007–6009.
[9] C. Hwang, A.J. Sinskey, H.F. Lodish, Oxidized redox state of glutathione in the endoplasmic reticulum, Science 257 (1992) 1496–1502.
[10] J.S. Stamler, A. Hausladen, Oxidative modifications in nitrosative stress, Nat. Struct. Biol. 5 (1998) 247–249.
[11] H. Yan, F. Huo, Y. Yue, J. Chao, C. Yin, Rapid reaction, slow dissociation aggregation, and synergetic multicolor emission for imaging the restriction and regulation of biosynthesis of Cys and GSH, J. Am. Chem. Soc. 143 (2021) 318–325.
[12] H. Appelqvist, P. Waster, K. Kagedal, K. Ollinger, The lysosome: from waste bag to potential therapeutic target, J Mol Cell Biol. 5 (2013) 214–226.
[13] F. Yu, Z. Chen, B. Wang, Z. Jin, Y. Hou, S. Ma, X. Liu, The role of lysosome in cell death regulation, Tumor Biol. 37 (2016) 1427–1436.
[14] N. Fehrenbacher, M. Jäättelä, Lysosomes as targets for cancer therapy, Cancer Res. 65 (2005) 2993–2995.
[15] B. Winchester, A. Vellodi, E. Young, The molecular basis of lysosomal storage diseases and their treatment, Biochem. Soc. Trans. 28 (2000) 150–154.
[16] X. Chen, Y. Zhou, X. Peng, J. Yoon, Fluorescent and colorimetric probes for detection of thiols, Chem. Soc. Rev. 39 (2010) 2120–2135.
[17] Y. Zhou, J. Yoon, Recent progress in fluorescent and colorimetric chemosensors for detection of amino acids, Chem. Soc. Rev. 41 (2012) 52–67.
[18] X. Zhang, X. Ren, Q. Xu, K.P. Loh, Z. Chen, One- and two-photon turn-on fluorescent probe for cysteine and homocysteine with large emission shift, Org. Lett. 11 (2009) 1257–1260.
[19] A. Poirel, A.D. Nicola, R. Ziessel, Thiazolidine derivatives from fluorescent dithienyl-BODIPY-carboxaldehydes and cysteine, J. Org. Chem. 79 (23) (2014) 11463–11472.
[20] H. Li, J. Fan, J. Wang, M. Tian, J. Du, S. Sun, P. Sun, X. Peng, A fluorescent chemodosimeter specific for cysteine: effective discrimination of cysteine from homocysteine, Chem. Commun. 39 (2009) 5904–5906.
[21] C. Han, H. Yang, M. Chen, Q. Su, W. Feng, F. Li, Mitochondria-targeted near-infrared fluorescent off-on probe for selective detection of cysteine in living cells and in vivo, ACS Appl. Mater. Interfaces. 7 (2015) 27968–27975.
[22] Y. Qi, Y. Huang, B. Li, F. Zeng, S. Wu, Real-time monitoring of endogenous cysteine levels in vivo by near-Infrared turn-on fluorescent probe with large Stokes shift, Anal. Chem. 90 (2018) 1014–1020.
[23] Y. Zhang, Y. Zhang, Y. Yue, J. Chao, F. Huo, C. Yin, Based on morpholine as luminescence mechanism regulation and organelle targeting dual function Cys NIR specific biological imaging probe, Sens. Actuators, B 320 (2020) 128348–128356.
[24] S. Girouard, M.‐ l. Houle, A. Grandbois, J.W. Keillor, S.W. Michnick, Synthesis and characterization of dimaleimide fluorogens designed for specific labeling of proteins, J. Am. Chem. Soc. 127 (2005) 559–566.
[25] M.A. R. Raycroft, K.É. Racine, C.N. Rowley, J.W. Keillor, Mechanisms of alkyl and aryl thiol addition to N-methylmaleimide, J. Org. Chem. 83 (2018) 11674–11685.
[26] Y. Ma, W. Gao, L. Zhu, Y. Zhao, W. Lin, Development of a unique reversible fluorescent probe for tracking endogenous sulfur dioxide and formaldehyde fluctuation in vivo, Chem. Commun. 55 (2019) 11263–112266.
[27] B. Shen, W. Zhu, X. Zhi, Y. Qian, A lysosome targeting probe based on fluorescent protein chromophore for selectively detecting GSH and Cys in living cells, Talanta 208 (2020) 120461–120469.
[28] X. Chen, L. Niu, N. Shao, Q. Yang, BODIPY-based fluorescent probe for dual-channel detection of nitric oxide and glutathione: visualization of cross-talk in living cells, Anal Chem. 91 (2019) 4301–4306.
[29] D. Yu, F. Huang, S. Ding, G. Feng, Near-infrared fluorescent probe for detection of thiophenols in water samples and living cells, Anal. Chem. 86 (2014) 8835–8841.
[30] X. Wu, X. Sun, Z. Guo, J. Tang, Y. Shen, T.D. James, H. Tian, W. Zhu, In vivo and in situ tracking cancer chemotherapy by highly photostable NIR fluorescent theranostic prodrug, J. Am. Chem. Soc. 136 (2014) 3579–3588.
[31] X. Li, Y. Hou, J. Zhao, J. Li, S. Wang, J. Fang, Combination of chemotherapy and oxidative stress to enhance cancer cell apoptosis, Chem. Sci. 11 (2020) 3215–3222.
[32] W. Zhang, W. Gu, T. Cheng, B. Wang, Y. Jiang, J. Shen, A novel near-infrared and naked-eyes turn on fluorescent probe for detection of biothiols with a large Stokes shift and its application in living cells, Anal. Methods 10 (2018) 3991–3999.
[33] L. Fan, W. Zhang, X. Wang, W. Dong, Y. Tong, C. Dong, S. Shuang, A two-photon ratiometric fluorescent probe for highly selective sensing of mitochondrial cysteine in live cells, Analyst. 144 (2019) 439–447.
[34] J. Liu, Y. Sun, Y. Huo, H. Zhang, L. Wang, P. Zhang, D. Song, Y. Shi, W. Guo, Simultaneous fluorescence sensing of Cys and GSH from different emission channels, J Am Chem Soc. 136 (2014) 574–577.
[35] X. Song, Y. Yang, J. Ru, Y. Wang, F. Qiu, Y. Feng, G. Zhang, W. Liu, Highly specific monitoring and imaging of endogenous and exogenous cysteine in living cells, Talanta 204 (2019) 561–568.
[36] Y. Long, J. Liu, D. Tian, F. Dai, S. Zhang, B. Zhou, Cooperation of ESIPT and ICT processes in the designed 2-(2'-hydroxyphenyl)benzothiazole derivative: a near-infrared two-photon fluorescent probe with a large stokes shift for the detection of cysteine and its application in biological environments, Anal Chem. 92 (2020) 14236–14243.
[37] S. Cai, C. Liu, X. Jiao, L. Zhao, X. Zeng, A lysosome-targeted near-infrared fluorescent probe for imaging endogenous cysteine (Cys) in living cells, J. Mater. Chem. B. 8 (2020) 2269–2274.
[38] C. Han, H. Yang, M. Chen, Q. Su, W. Feng, F. Li, Mitochondria-targeted near-infrared fluorescent off−on probe for selective detection of cysteine in living cells and in vivo, ACS Appl. Mater. Interfaces. 7 (2015) 27968–27975.
[39] Y. Yang, Y. Wang, Y. Feng, C. Cao, X. Song, G. Zhang, W. Liu, Light-driven visualization of endogenous cysteine, homocysteine, and glutathione using a near-infrared fluorescent probe, J. Mater. Chem. B. 7 (2019) 7723–7728.
[40] S. Li, D. Song, W. Huang, Z. Li, Z. Liu, In situ imaging of cysteine in the brains of mice with epilepsy by a near-infrared emissive fluorescent probe, Anal. Chem. 92 (2020) 2802–2808.
[41] Y. Yue, F. Huo, P. Yue, X. Meng, J.C. Salamanca, J.O. Escobedo, R.M. Strongin, C. Yin, In situ lysosomal cysteine-specific targeting and imaging during dexamethasone-induced apoptosis, Anal Chem. 90 (2018) 7018–7024.
[42] Z. Guo, S. Nam, S. Park, J. Yoon, A highly selective ratiometric near-infrared fluorescent cyanine sensor for cysteine with remarkable shift and its application in bioimaging, Chem. Sci. 3 (2012) 2760–2765.
[43] J. Ge, L. Fana, K. Zhang, T. Ou, Y. Li, C. Zhang, C. Dong, S. Shuang, M.S. Wong, A two-photon ratiometric fluorescent probe for effective monitoring of lysosomal pH in live cells and cancer tissues, Sens. Actuators, B 262 (2018) 913–921.
[44] C. Liu, R. Zhang, W. Zhang, J. Liu, Y. Wang, Z. Du, B. Song, Z. Xu, J. Yuan, "Dual-key-and-lock" ruthenium complex probe for lysosomal formaldehyde in cancer cells and tumors, J Am Chem Soc. 141 (2019) 8462–8472.

[45] S. Muthusamy, K. Rajalakshmi, D. Zhu, L. Zhao, S. Wang, W. Zhu, A novel lysosome targeted fluorophore for $H_2S$ sensing: Enhancing the quantitative detection with successive reaction sites, Sens. Actuators, B 320 (2020) 128443–128451.
[46] L. Shi, S. Yang, H. Hong, Y. Li, H. Yu, G. Shao, K. Zhang, S. Gong, A novel target and pH dual-activatable fluorescent probe for precisely detecting hypochlorite in lysosomes, Anal Chim Acta. 1094 (2020) 122–129.
[47] X. Zhang, N. He, Y. Huang, F. Yu, B. Li, C. Lv, L. Chen, Mitochondria-targeting near-infrared ratiometric fluorescent probe for selective imaging of cysteine in orthotopic lung cancer mice, Sens. Actuators, B 282 (2019) 69–77.
[48] J. Wang, B. Li, W. Zhao, X. Zhang, X. Luo, M.E. Corkins, S.L. Cole, C. Wang, Y. Xiao, X. Bi, Y. Pang, C.A. McElroy, A.J. Bird, Y. Dong, Two-photon near infrared fluorescent turn-on probe toward cysteine and its imaging applications, ACS Sens. 1 (2016) 882–887.